



Dammarane triterpenes targeting α -synuclein: biological activity and evaluation of binding sites by molecular docking

Alberto Cornejo, Julio Caballero, Mario Simirgiotis, Vanessa Torres, Luisa Sánchez, Nicolás Díaz, Marcela Guimaraes, Marcos Hernández, Carlos Areche, Sergio Alfaro, Leonardo Caballero & Francisco Melo

To cite this article: Alberto Cornejo, Julio Caballero, Mario Simirgiotis, Vanessa Torres, Luisa Sánchez, Nicolás Díaz, Marcela Guimaraes, Marcos Hernández, Carlos Areche, Sergio Alfaro, Leonardo Caballero & Francisco Melo (2021) Dammarane triterpenes targeting α -synuclein: biological activity and evaluation of binding sites by molecular docking, *Journal of Enzyme Inhibition and Medicinal Chemistry*, 36:1, 154-162, DOI: [10.1080/14756366.2020.1851216](https://doi.org/10.1080/14756366.2020.1851216)

To link to this article: <https://doi.org/10.1080/14756366.2020.1851216>



© 2020 The Author(s). Published by Informa UK Limited, trading as Taylor & Francis Group.



[View supplementary material](#)



Published online: 14 Dec 2020.



[Submit your article to this journal](#)



Article views: 1660



[View related articles](#)



[View Crossmark data](#)



Citing articles: 2 [View citing articles](#)

RESEARCH PAPER



Dammarane triterpenes targeting α -synuclein: biological activity and evaluation of binding sites by molecular docking

Alberto Cornejo^a, Julio Caballero^b, Mario Simirgiotis^c , Vanessa Torres^a, Luisa Sánchez^a, Nicolás Díaz^a, Marcela Guimaraes^d, Marcos Hernández^e, Carlos Areche^e , Sergio Alfaro^f, Leonardo Caballero^g and Francisco Melo^g

^aEscuela de Tecnología Médica, Facultad de Medicina, Universidad Andres Bello, Laboratorio Catem V, Santiago, Chile; ^bDepartamento de Bioinformática, Facultad de Ingeniería, Centro de Bioinformática, Simulación y Modelado (CBSM), Universidad de Talca, Talca, Chile; ^cFacultad de Ciencias, Instituto de Farmacia, Universidad Austral de Chile, Valdivia, Chile; ^dDepartment of Science and Technology, Federal University of São Paulo, São José dos Campos, Brazil; ^eDepartamento de Química, Facultad de Ciencias, Universidad de Chile, Santiago, Chile; ^fDoctorado en Ciencias, mención Modelado de Sistemas Químicos y Biológicos, Centro de Bioinformática, Simulación y Modelado (CBSM), Facultad de Ingeniería, Universidad de Talca, Talca, Chile; ^gDepartamento de Física and Soft Matter Research Center, SMAT-C, Universidad de Santiago, Santiago, Chile

ABSTRACT

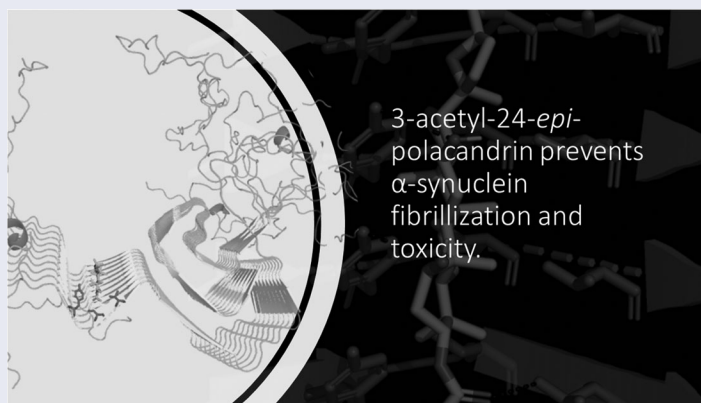
Parkinson's disease (PD) is a neurodegenerative disorder that affects adult people whose treatment is palliative. Thus, we decided to test three dammarane triterpenes **1**, **1a**, **1b**, and we determined that **1** and **1a** inhibit β -aggregation through thioflavine T rather than **1b**. Since compound **1** was most active, we determined the interaction between α -synuclein and **1** at 50 μ M (Kd) through microscale thermophoresis. Also, we observed differences in height and diameter of aggregates, and α -synuclein remains unfolded in the presence of **1**. Also, aggregates treated with **1** do not provoke neurites' retraction in N2a cells previously induced by retinoic acid. Finally, we studied the potential sites of interaction between **1** with α -synuclein fibrils using molecular modelling. Docking experiments suggest that **1** preferably interact with the site 2 of α -synuclein through hydrogen bonds with residues Y39 and T44.

ARTICLE HISTORY

Received 29 July 2020
Revised 9 November 2020
Accepted 10 November 2020

KEYWORDS

Parkinson's disease;
oligomers; drug target;
natural compounds modifiers




Introduction

The protein α -synuclein is a 14 kDa protein that belongs to the family of synucleins. It has been associated with neurodegenerative disorders, and it is found in high concentrations in presynaptic terminals, associated with the reserve pool of synaptic vesicles^{1,2}. This protein has been associated with synaptic vesicle recharge and trafficking from the reserve pool to its release, interacting with proteins that control vesicle exocytosis, such as the family of small RAB GTPases, phospholipase D2, and promoting

the SNARE complex, which is directly involved in the release of neurotransmitters, including dopamine³. Its structure is divided into three regions; the N-terminal region, characterised by having 11 repetition domains of seven amino acids giving as a secondary structure alpha amphipathic helix⁴.

Between the amino acids, 61–95 resides the NAC region, known as the non-amyloid- β component, highly hydrophobic, is indispensable for aggregation. The elimination of large segments of this region dramatically decreases fibrillogenesis. Finally, the C-terminal region is structured by negatively charged amino acids,

CONTACT Alberto Cornejo  alberto.cornejo@unab.cl  Escuela de Tecnología Médica, Facultad de Medicina, Universidad Andres Bello, Laboratorio Catem V, Echaurren 183, Santiago, Chile.

 Supplemental data for this article can be accessed [here](#).

© 2020 The Author(s). Published by Informa UK Limited, trading as Taylor & Francis Group.

This is an Open Access article distributed under the terms of the Creative Commons Attribution License (<http://creativecommons.org/licenses/by/4.0/>), which permits unrestricted use, distribution, and reproduction in any medium, provided the original work is properly cited.

resulting in a polar region¹. This protein is encoded on chromosome 4 q21 (SNCA gene)⁵, whose point mutations are located predominantly in the N-terminal region as A30P, E46K, A53T, and some recently described G51D and H50Q, associated with different PD varieties⁶.

Moreover, α -synuclein is prone to form aggregates and subsequently leads to the formation of amyloid deposits. In Parkinson's disease (PD), α -synuclein aggregates can be found in dopaminergic neurons as self-misfolding protein inclusions known as Lewy bodies⁷. More importantly, this folding can form oligomers, which have a toxic effect on the neuronal membrane, altering permeability, causing an influx of calcium, depolarising the membrane. Also, oligomers can cause oxidative damage leading to cell death⁸. This neurodegenerative disorder's hallmark is characterised by the accumulation of intraneuronal inclusions composed of α -synuclein rich in β -sheet. These inclusions' neurotoxicity could influence other proteins to lose their function, having a role structure such as prefibrillar species, which might be toxic to neurons¹. In PD, the primary treatment is levodopa (L-DOPA). However, several studies have found side effects in patients who use this medication, including nausea, vomiting, and significant movement disorders. These symptoms can increase in frequency if L-DOPA loses its effect. Also, catechol-O-methyl transferase (COMT) inhibitors are a ubiquitous enzyme that catalyses the O-methylation catechol-containing substrates by transferring, in the presence of magnesium, a methyl group from S-adenosylmethionine. The methylation is essential to discard biologically active or toxic catechols and some other hydroxylated metabolites⁹. Moreover, inhibitors such as opicapone have a typical structure: (3,4-dihydroxy-5-nitrophenyl), suggesting that this structure can increase systemic and central L-DOPA bioavailability¹⁰.

Along with the mechanism of action, substantial evidence indicates that it causes low secondary effects for Parkinson's patients, contrasting with other COMT inhibitors, more commonly used like tolcapone¹¹. Moreover, several approaches have risen to focus on the clearance of toxic deposits, promoting proteasomal activity, and targeting the inhibition of α -synuclein aggregates¹². Interestingly, the polyphenol (-)-epigallocatechin gallate redirects amyloid fibril formation of α -synuclein into a non-pathogenic pathway¹³.

In the present work, we demonstrated that dammarane triterpene **1** inhibits aggregates progression of α -synuclein (50 μ M Kd) through hydrogen bonds from hydroxyl and carbonyl groups of compound **1**. Moreover, α -synuclein, after 48 h of aggregation in the presence of **1** it remains unfolded, demonstrated through Raman spectroscopy experiments. Then, we demonstrated that oligomers in the presence of **1** did not exert neurite retraction in N2a cells instead of aggregates untreated that exert a deleterious effect on cells. Ultimately, we show how **1** interacts with α -synuclein fibrils that interact with different sites, evidentiating that compounds such as dammarane triterpenes may serve as a scaffold for exploring new drug design for PD.

Materials and methods

Chemistry

Silica gel (Kieselgel 60, Merck, Darmstadt, Germany, 0.063–0.200 mm) and Sephadex LH-20 were used in column chromatography (CC). Solvents used in extraction were previously distilled and dried according to standard procedures. The extraction and purification of **1**, **1a**, and **1b** were carried out mainly as described¹⁴. The purity of all compounds was estimated by using

an HPLC-PDA ($\geq 98\%$) (Agilent LC-1200, Santa Clara, CA). α -recombinant protein was purified by HPLC and, ThT assays were performed in a Biotek H1. The dissociation constant (Kd) was determined through microscale thermophoresis (MTS). The atomic force images were obtained using a Nanoscope III equipment in tapping mode. The Raman spectra and maps were obtained through a Confocal Raman Microscopy Alpha 300 (WITec GmbH, Ulm, Germany).

Extraction and isolation. The air-dried aerial parts of *Ibicella lutea* from the Province of Mendoza (2.5 kg) were extracted with CHCl_3 to obtain after evaporation of the solvent, 105 g of extract¹⁴. The CHCl_3 extract (50 g) was fractionated by vacuum-liquid chromatography (VLC) over silica gel 60H (Merck, Darmstadt, Germany). The fraction eluted with 50% EtOAc (5 g) was then chromatographed on HPLC reversed-phase silica gel with MeOH-H₂O (7:3, v:v), and recrystallisation from CH_3CN , to afford compound **1** (1 β -acetoxi-20(S), 24(R)-epoxi-3 α , 12 β , 25-trihydroxidammarane, 230 mg).

Hydrolysis of compound 1. Compound **1** (10 mg) was added to a solution of 10% KOH in MeOH (5 ml) under argon, and the mixture was stirred at room temperature for 8 h. Then, 2 ml of the solvent was evaporated, and the remaining solution was poured into a mixture of 5 g of ice and 10 ml of 1 M HCl. The mixture was extracted with EtOAc (2 \times 10 ml). The combined extracts were washed with brine (10 ml), dried over Na_2SO_4 , and concentrated under reduced pressure to give a residue, which was purified by HPLC (NP column, 300 \times 8 mm, EtOAc-hexane (9:1), flow rate: 1.0 ml) to afford **1a** 20(S), 24(R)-epoxi-1 β , 3 α , 12 β , 25-tetrahydroxidammarane, 24-epi-polacandrin¹⁴ (7 mg, 70% yield, Rf 0.35 in EtOAc).

Acetylation of 1. Compound **1** (25 mg) was dissolved in a mixture of pyridine (1 ml) and Ac_2O (3 ml) with a catalytic amount of DMAP, and the mixture was heated under reflux in a glycerine bath for 3 h. The reaction mixture was then concentrated under reduced pressure and, after the usual workup procedure and purification by HPLC (NPcolumn, 300 \times 8 mm, EtOAc-hexane (7:3), flow rate: 1.0 ml), gave the peracetylated compound **1b** 1 β ,3 α , 12 β 25-tetracetoxi-20(S), 24(R)-epoxidammarane¹⁴.

α -Synuclein expression and purification

The sequence of WT α -synuclein inserted into plasmid pT7-7 was donated gently by Dr. Claudio Fernández (Rosario, Argentina). This fragment was cloned into the pET-28a vector (Novagen) to produce a His-tagged protein expressed in *Escherichia coli* strain BL21 (DE3). LB medium containing kanamycin (30 μ g/ml) was inoculated with a stationary overnight culture. The culture was grown at 37 °C to OD 600 of 0.4–0.6, and protein expression was induced by the addition of 1 mM IPTG for 4 h. The cells were pelleted and sonicated. Recombinant α -synuclein was purified via ProPac IMAC 10 (Thermo Fisher Scientific, Waltham, MA) using a gradient of 10–200 mM imidazole, 20 mM Na_2HPO_4 , and 500 mM NaCl. The purity of the protein was verified on a Coomassie Brilliant Blue-stained SDS-polyacrylamide gel. The protein was concentrated and stored at –80 °C until use. The concentration was determined using the extinction coefficient at 275 nm (5600 $\text{M}^{-1} \text{cm}^{-1}$) as described¹⁵.

α -Synuclein aggregation and ThT measurements

Thirty micromolar of α -synuclein in 25 mM Na_2HPO_4 were incubated at 37 °C in constant shaking at 300 rpm for 48 h into Eppendorf tubes to form aggregates. To ThT fluorescence

measurement concentration of ThT was adjusted to 25 μM , after 1 h of incubation at 37 °C, the plates were read in a Biotek H1 multi-mode reader in a 96-black plate flat bottom. The Ex/Em was set at 440/485 nm.

Microscale thermophoresis

Microscale thermophoresis assays were performed on a Premium MonolithTM NT.115 microscale thermophoresis device (NanoTemper, Munich, Germany) after labelling the protein RED-NHS dye as specified by the manufacturer. Assays were performed in 50 mM phosphate buffer (pH 8.0) supplemented with 0.05% Tween-20 using 20 nM labelled protein and inhibitor concentrations varying between 750 μM and 0.02 μM . Samples were incubated 10 min at room temperature before loading the assay capillaries. Data were analysed with PALMIST¹⁶.

Raman spectra acquisition and spectral processing

The samples, 3 μl , were placed on a slide and left to dry at room temperature. The acquisition was made through a Raman confocal microscope equipped with a laser with a wavelength of 532 nm and a CCD camera cooled to -60 °C. A single-mode optical fibre was used to connect the laser to a $\times 100$ lens. The laser power was set to 10 mW. Each spectrum was obtained by averaging 10 accumulations with an acquisition time of 30 s for each accumulation, using WiTec's Control Four software. The scanned images, a matrix of 20 dots per line was established on a surface of 5 μm (width) and 5 μm (height), with an integration time of 5 s per spectrum. The spectral processing was performed using Matlab. The bands' intensities are normalised to the 1100 cm^{-1} bands' average intensity corresponding to the glass. Then, the spectral contribution of the glass was subtracted numerically. The Raman intensity was analysed by filtering peaks through the Lorentzian function. Raman acquisition was repeated in triplicate.

AFM images in tapping mode

AFM imaging was performed in tapping (intermittent contact) mode using a Nanoscope III (Veeco, Santa Barbara, CA) and Si_3N_4 cantilevers (NPS series, Veeco, Santa Barbara, CA) exhibiting spring constants of 40–60 N/m at resonance frequencies of 6–10 kHz as described¹⁷. Briefly, α -synuclein 30 μM was diluted in 10 mM Tris-HCl, pH 7.4, 50 mM KCl, and then immobilised onto mica freshly cleaved to a final concentration of 5 μM . A drop of α -synuclein protein solution was adsorbed for 30 min. The excess of protein was removed by washing with 10 mM Tris-HCl, pH 7.4, and 50 mM KCl solution.

N2a cell culture

N2a neuroblastoma cells were cultured at 37 °C in a humidified atmosphere at 5% CO_2 , using MMM Group[®] Stove, Standard CO_2 Cell 190, in DMEM D1152 plus F-12 medium supplemented with 10% bovine foetal serum[®] Biowest, 100 $\mu\text{g}/\text{ml}$ ampicillin and 100 $\mu\text{g}/\text{ml}$ streptomycin, in T25 cell culture flasks. To the differentiation procedure, cells were cultured in Petri dishes 35/10 mm over coverslips, then was added SFB at 2.5% plus retinoic acid of 10 μM for five days replacing medium culture every 48 h for neurite grown monitored through an inverted microscope. Either aggregates alone or aggregates treated with **1** at 30 nM were added at day 4 for 24 h in the culture medium. After that, cells were fixed for immunofluorescence. The cells were then washed twice with

1 \times PBS buffer (137 mM NaCl, 10 mM Na_2HPO_4 , 2.7 mM KCl, 1.76 mM KH_2PO_4), fixed for 30 min with 4% paraformaldehyde at room temperature, washed three times with PBS, and permeabilised for 10 min with Triton X100 0.5% (Sigma-Aldrich, St. Louis, MO) diluted in PBS. Finally, coverslips were washed three times with PBS. After that, cells were incubated with a 1% BSA (Sigma-Aldrich, St. Louis, MO) for 30 min at room temperature. Subsequently, samples were incubated at 37 °C for one hour with the supernatant of α tubulin monoclonal TU-01 kindly donated by Dráber and coworkers^{18,19}, then diluted in blocking solution 0.1% BSA and washed three times in PBS. After that, cells were incubated with Alexa Fluor 488 Goat anti-Mouse IgG (Thermo Fisher Scientific, Waltham, MA) for one hour at room temperature and washed three times in PBS. Subsequently, the cells were mounted 4',6-diamidino-2-phenylindole (Vectashield, Vector, Burlingame, CA). Samples were analysed in a confocal microscope, Zeiss LSM Meta (Oberkochen, Germany).

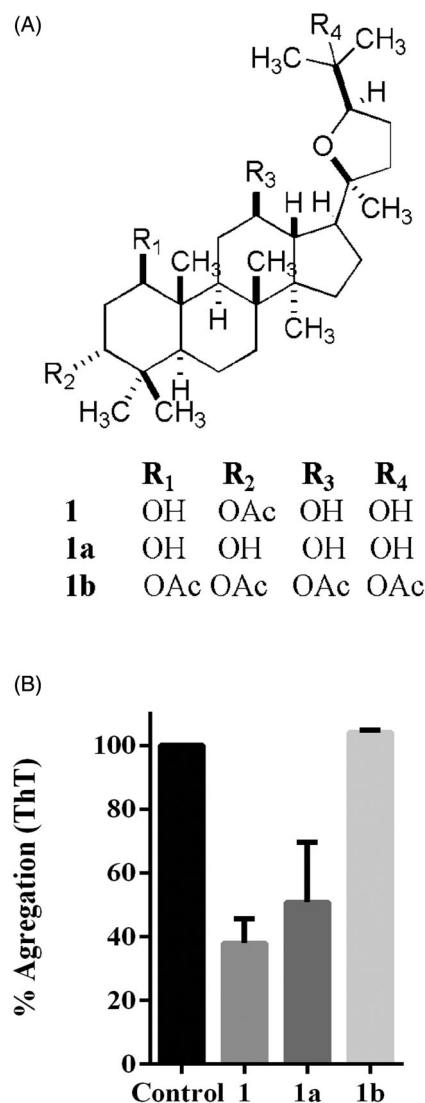


Figure 1. (A) Compound **1** is 3 α -acetoxi-20(S), 24(R)-epoxi-1 β , 12 β , 25-trihydroxidammarane, named 3 α -acetyl-24-*epi*-polacandrin **1a** is the hydrolysis product of **1**, and compound **1b** is its peracetylated derivative. (B) Thioflavine T experiment at 48 h. Significance was determined with ANOVA with Dunnett's test at $p < 0.05$.

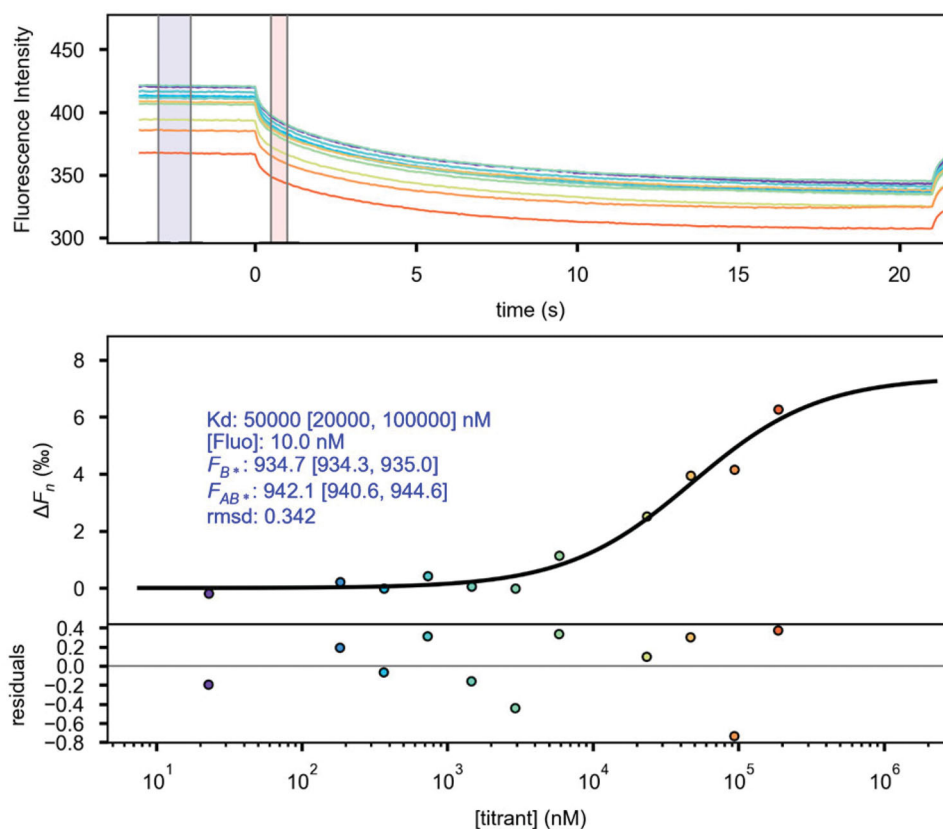


Figure 2. Dissociation constant (K_d) measured in the presence of **1**. (A) Graphical representation of time versus fluorescence. (B) Dose-response graph of the corresponding thermophoresis measurements shown in (A).

Molecular docking

The structure of full-length α -synuclein fibrils has been resolved by solid-state NMR (protein data bank code 2N0A)²⁰. This model contains 10 units of the peptide (140 amino acids), which are arranged in parallel by presenting features that commonly stabilise amyloid folds (such as intermolecular salt bridge, a glutamine ladder, steric zippers involving hydrophobic residues, and in-register parallel- β -sheet hydrogen-bonding with a Greek key motif). In a recent report, Hsieh et al. used this structure as a target protein for molecular blind docking of small molecules²¹. They found 13 putative binding sites, but they excluded a number of these sites based on their low percent probability of interaction; finally, they identified site 2 (with residues Y39, S42, and T44), site 9 (with residues G86, F94, and K96), and the site 3/13 (with residues L43, L45, V48, and H50)²¹. Docking calculations were executed inside these sites by using Glide XP method²². The structures of **1**, **1a**, and **1b** were sketched using Maestro's molecular editor (Maestro 10.2.011, Schrödinger LLC, New York, NY). Grid boxes of $25 \text{ \AA} \times 25 \text{ \AA} \times 25 \text{ \AA}$ were defined in the centre of these sites. Docking parameters were used as in previous works^{23,24}. The docking protocol begins with the systematic ligand conformational search followed by its placement in the receptor sites. Minimisation was performed by using the OPLS-AA²⁵ force field (distance-dependent dielectric = 2.0). Further, a Monte Carlo algorithm samples the nearby torsional minima of the lowest energy poses. According to the energies ranked by GlideScore, the more favourable conformations were selected as the best poses.

The stability of the identified docked poses was done using molecular dynamics (MD) simulation with the model of α -synuclein fibrils forming complexes with compound **1** (3 units) in sites 2, 9, and 3/13, respectively, since compound **1** was the most

potent inhibitor. Desmond v3.5 software was used with the OPLS-AA force field^{25,26}. The complex was solvated to construct a $112 \text{ \AA} \times 140 \text{ \AA} \times 100 \text{ \AA}$ water box. Na^+ and Cl^- ions were added to replicate physiological conditions and guarantee that the whole system was neutral. Simulation parameters were established as described here: an NPT ensemble was used, the constant temperature at 300 K was imposed by using the Nosé-Hoover chain thermostat, and constant pressure at 1 atm was imposed by using the Martyna-Tobias-Klein barostat. RESPA integrator was applied with a 2-fs time step for bonded and nonbonded-near forces and 6 fs for long-range forces. Particle-mesh Ewald with a 9 \AA cut-off radius was employed for long-range electrostatics. The protein backbone was restrained with a constant force of $5 \text{ kcal mol}^{-1} \text{ \AA}^{-2}$. In the beginning, a 20-ns MD simulation was performed to equilibrate the system, and then the production MD was performed for 150 ns.

Data analysis

The Raman spectra analysis was done by using Matlab software (Natick, MA), and the statistical analysis was done by using GraphPad 7 (La Jolla, CA).

Results

Effect of **1** over α -synuclein aggregation

The isolation of **1**, and further derivatives **1a**, **1b** (Figure 1(A)) were tested as α -synuclein inhibitors through fluorescent probe thioflavine T, which has a high affinity for fibrils amyloids²⁷. Thus, we decided to induce aggregation for 48 h of α -synuclein. Then,

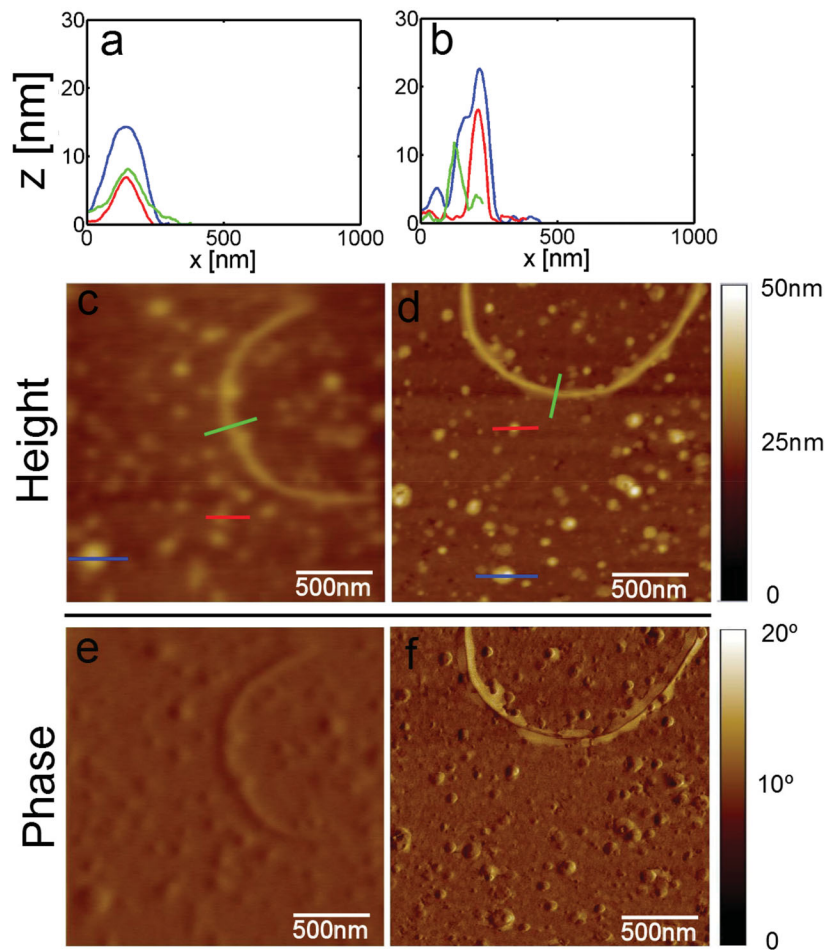


Figure 3. Atomic force microscopy images of α -synuclein aggregates represented as control of aggregation, height, and phase are depicted.

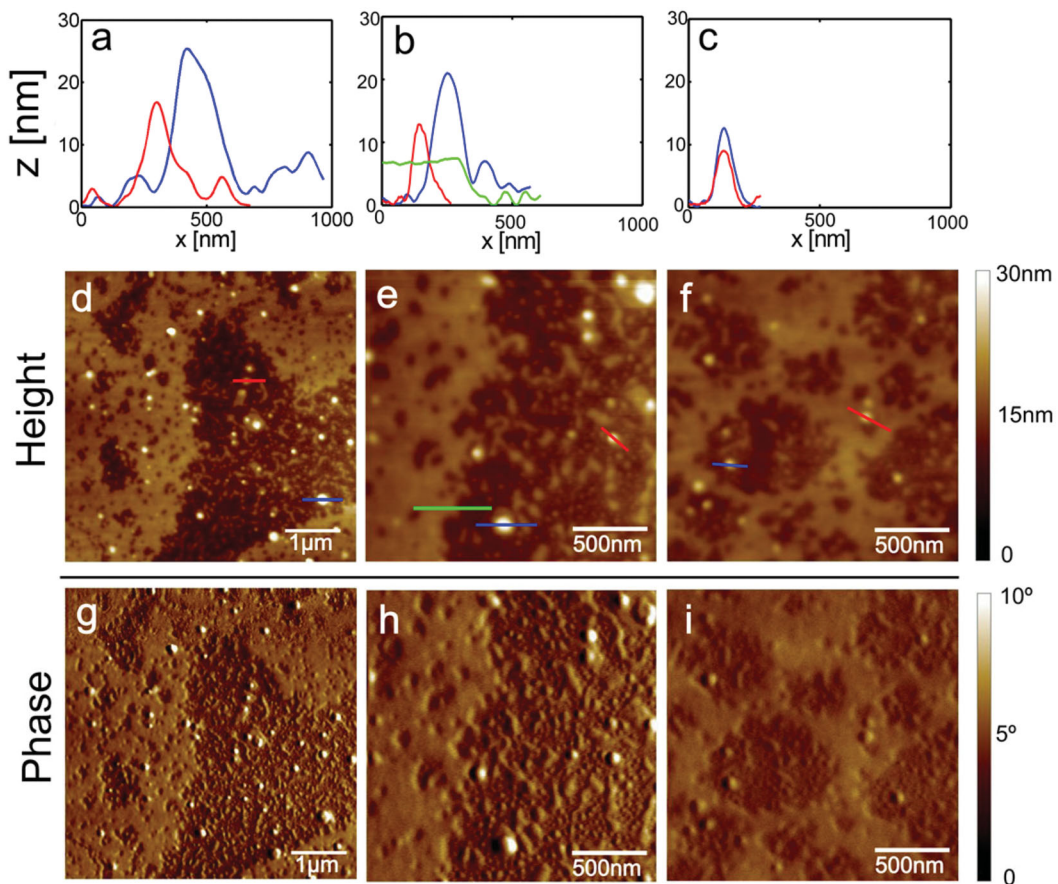


Figure 4. Atomic force microscopy images of α -synuclein aggregates in the presence of 1, height, and phase are depicted.

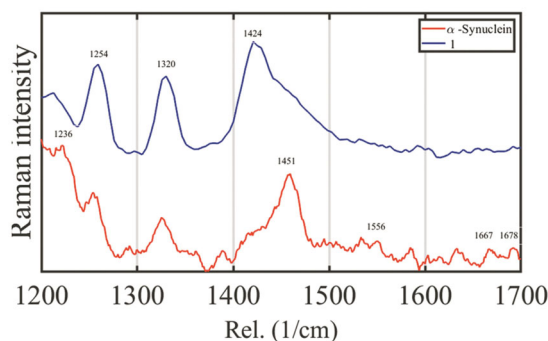


Figure 5. Raman spectroscopy of α -synuclein after 48 h of incubation in the absence or presence of **1**. Raman spectra were recorded, including regions amide I, II, and III, in the control of aggregation (red spectra) and only amide III in α -synuclein (blue spectra).

we assayed the three compounds against fibril formation. Thus, compounds **1** and **1a** at 100 μ M shown inhibition activity into the assembly of β -sheet since there is a diminishing in fluorescence intensity. Interestingly, the peracetylated compound **1b** did not exert inhibition against the assembly of β -sheet, suggesting that hydroxyls and acetyl group in compound **1** play a role in the inhibition of fibril formation (Figure 1(B)). Thermophoresis (TMS) is known as the Soret effect, and it is an analytical method introduced as an alternative to studying interactions between protein and small compounds²⁸. The Soret effect corresponds to the mobility of the particles under the influence of a gradient of temperature. Thus, we decided to determine the interaction between α -synuclein and **1**; our results of the dissociation constant (Kd) was 50 μ M, considering that this technique was designed to study non-covalent interactions such as hydrogen bonds that might be involved in the interaction between α -synuclein and **1** (Figure 2(A,B)).

The aggregation process reveals morphological and amide region pattern changes after treatment with **1**.

Then, we performed atomic force microscopy (AFM) experiments to corroborate the effect of **1** on α -synuclein aggregation. The tapping mode on mica provides the phase information, making it possible to distinguish morphological differences between the samples. Besides, AFM images in the tapping mode allow for the determination of topographic details, verifying its thickness using a cross-section obtained from the topographic image showing the distribution of elements. In control experiments, elements such as oligomers and fibrils are presents, whose height is about 15 nm, while in treated aggregates, the height is about 5 nm. Moreover, the diameter of treated aggregates is ranging from 180 to 400 nm. However, the control experiment aggregates have a diameter distributed under 200 nm (Figures 3 and 4 and Supplementary Figure S1), suggesting different pathways in these aggregates' conformation.

Raman spectroscopy experiments reveal that upon α -synuclein aggregation, we observed bands belonging to the amide I region related to C=O stretch at 1667 cm^{-1} , associated with β sheet content. It also arises from the same region, a band at 1674 cm^{-1} belonging to polyproline II²⁹. In the amide region II related to C-N stretch and N-H bend, there is a band at 1556 cm^{-1} associated with β -sheet content. In the amide region III, whose vibrational modes are associated with C-N stretch and N-H bending, a band at 1236 cm^{-1} arises linked with a β -sheet secondary structure. There are two bands at 1320 and 1451 cm^{-1} related to CH₂ deformation and CH₂ and CH₃ deformation, respectively, as

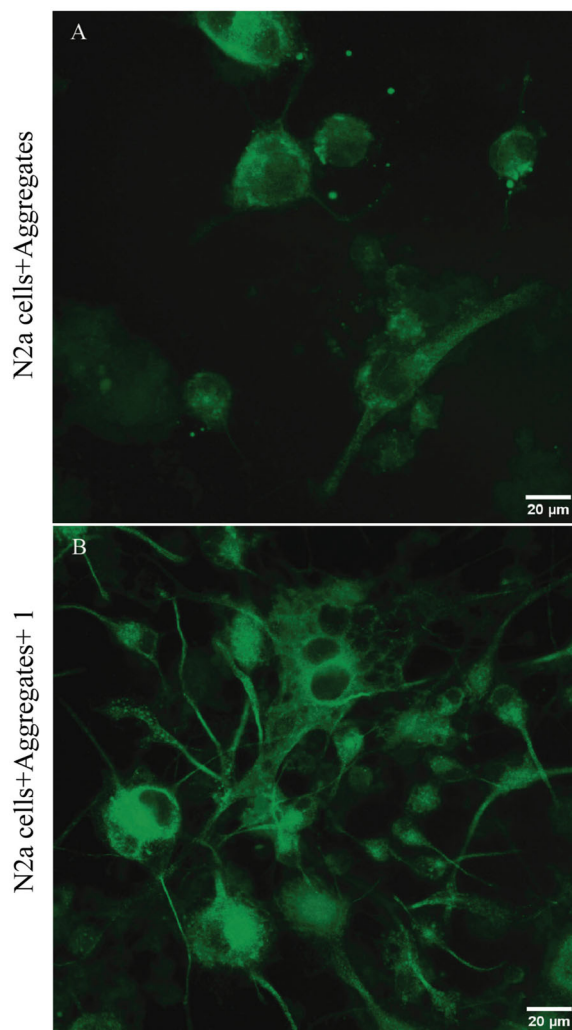


Figure 6. (A) α -synuclein aggregates (30 nM) incubated for 24 h in previously neurite-like structure induced by retinoic acid in N2a cells. (B) α -synuclein aggregates + **1** (30 nM) incubated for 24 h in previously neurite-like structure induced by retinoic acid in N2a cells. Bars 20 μ m.

previously described²⁹. Once we analysed the Raman spectra of α -synuclein in the presence of **1**, we found bands most associated with the amide III region, which includes bands at 1320 and 1424 cm^{-1} representing CH₂ deformation and CH₂ and CH₃ deformation, respectively. Also, we found a massive band at 1254 cm^{-1} that mostly represents random or unfolded protein. Thus, once we found a typical distribution representing α -synuclein aggregates, including bands associated with β -sheet, and the case of α -synuclein treated with **1** remains unfolded (Figure 5).

N2a cells preserve their neurite outgrow in the presence of treated aggregates by **1**.

Several pieces of evidence show that aggregates of α -synuclein could severely compromise the dopaminergic terminal and axons, leading to cell death³⁰. Therefore, we decided to investigate whether externally added aggregates to cell culture could provoke damage to N2a cells. Thus, we induced neurite extension through retinoic acid to resemble neurite-like outgrow (Supplementary Figure S2). Then, we incubated extracellular aggregates treated or not of compound **1** at 30 nM. Further, we observed that in N2a cells in the presence of α -synuclein aggregates, most of the cells retract their neurite extension and provoke cell swelling (Figure 6(A)).

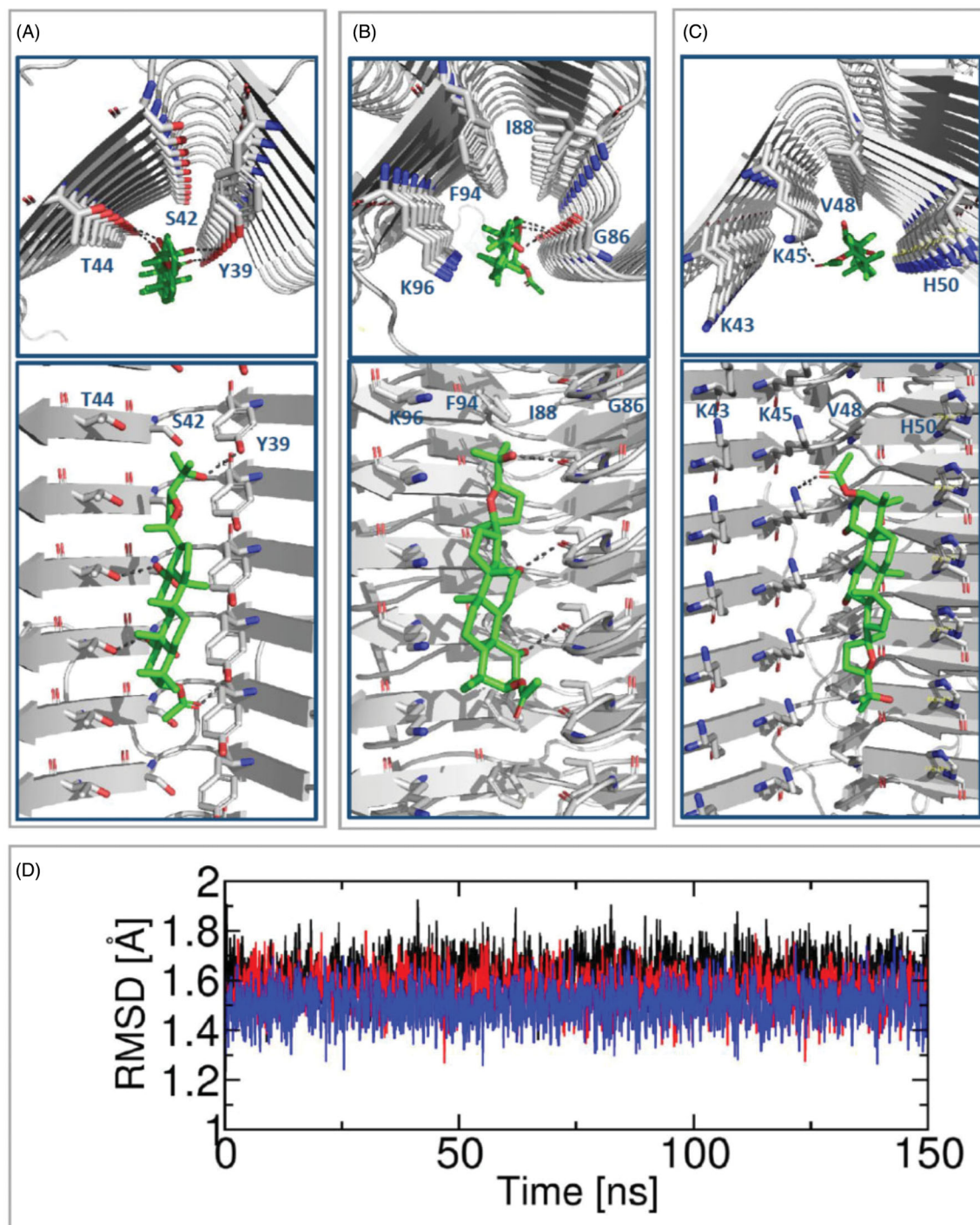


Figure 7. Molecular modelling studies of **1** forming complex with sites of α -synuclein. (A) Docking in site 2; (B) docking in site 9; (C) docking in site 3/13 (docked poses are viewed from the fibril axis at the top and are viewed from the fibril side view at the bottom, α -synuclein is in the grey cartoon). (D) RMSD of **1** in the sites 2 (black), 9 (blue), and 3/13 (red) from a 150-ns MD simulation.

Further, once we challenged N2a cells in the presence of the aggregated treated with **1**, the cells mostly preserve their neurite like-structure, as shown in Figure 6(B).

Elucidation of binding sites by **1** through molecular docking

Finally, to elucidate the potential binding sites, the docking results for **1** inside sites 2, 9, and 3/13 of α -synuclein fibrils are shown in Figure 7(A–C). The obtained models suggest that **1** is capable of binding to these sites. However, the scoring energies are more

favourable for the interaction with site 2 (scoring energies for the sites 2, 9, and 3/13 had values of -4.617 , -2.545 , and -2.592 kcal/mol, respectively). The most energetically favourable docking pose of **1** extends along with site 2, where hydroxyl and carbonyl groups of the ligand form hydrogen bonds with the side chains of several Y39 and T44 residues (Figure 7). Docking experiments revealed that small compounds could display preferences for different sites²¹. The docking poses' stability was tested by performing a 150-ns MD simulation of the system that contains the three sites occupied by compound **1**. This simulation revealed that

compound **1** remained stable in the three sites since root-mean-square deviations (RMSDs) had almost constant values during the MD trajectory (Figure 7(D)). Our results indicate that **1** fit into the three explored sites since it has a good shape and can form stable chemical interactions.

Atomistically, the destabilisation of toxic α -synuclein oligomers by interacting with small molecules should proceed by complex mechanisms³¹. In these mechanisms, it is reasonable that the first step is to recognise the small molecule in sites of α -synuclein fibrils. Our docking results for complexes between dammarane triterpenes and α -synuclein fibrils represent the possible recognition sites that initiate this process. The elucidation of the complete mechanism, produced on large timescales, should consider that disruption of the fibrils' integrity induces significant conformational changes in the protein framework.

The docking poses for derivatives **1a** and **1b** inside the sites 2, 9, and 3/13 of α -synuclein fibrils were also obtained to explain the more significant inhibitory activity of compound **1**. The energies of binding and the description of the α -synuclein residues that form hydrogen bond interactions with these compounds are depicted in Supplementary Table S1 and Figure S3. Docking results revealed that compound **1** had the most favourable energy value in site 2 (with scoring energy of -4.617 kcal/mol as mentioned above). In comparison, compounds **1a** and **1b** had scoring energies of -4.286 kcal/mol (inside site 9) and -3.702 kcal/mol (inside site 2). The calculated energy trend is in agreement with the experimental activity trend. The analysis of the complexes' structural features, specifically the intermolecular hydrogen bonds, allows explaining the differential activity of the three dammarane triterpenes **1**, **1a**, and **1b**. The substituents in compound **1** ($R_1=OH$, $R_2=OAc$, $R_3=OH$, and $R_4=OH$) can establish hydrogen bonds with two Y39 and two T44 residues inside site 2 (Figure 7). When OH replaces OAc in R2 in compound **1a**, and when OAc replaces OH in R4 in compound **1b**, one of the hydrogen bond interactions with T44 is lost. This analysis indicates that compound **1** has optimal substituents for establishing hydrogen bond interactions with α -synuclein fibrils.

Discussion

Among the neurodegenerative disorders, PD is the fastest-growing neurodegenerative disorder after Alzheimer's disease affecting older people worldwide. The global burden is around 6.2 million people affected, whose number will be increasing around 13 million by 2040³². The standard treatment is the use of L-DOPA; however, there are several side effects. PD's pathological hallmark is α -synuclein aggregates, whose NAC region involves a hydrophobic region responsible for its fibrillisation³³. In this regard, several compounds interfere in different ways, either stabilising the monomer or preventing the fibrillisation³¹. Thus, avoiding the formation of these aggregates appears as an alternative for drug development.

Interestingly, a polyphenol (–)-epigallocatechin gallate redirects the amyloid pathway preventing the formation of structures rich in β -sheet conformation through hydrogen bonds³⁴. Moreover, these non-toxic elements do not provoke cytotoxicity in PC12 cells¹³. Moreover, baicalein, a natural flavonoid, can prevent fibrillisation and disassembly of existing fibrils through the interaction of o-quinone with lysine forming a Schiff base³⁴. Interestingly, baicalein can protect dopaminergic neurons in mice^{35,36}.

Besides, some compounds containing a nitro-catechol moiety arise as alternatives for PD treatment by slowing dopamine degradation⁹. Moreover, compounds such as entacapone and

tolcapone inhibit fibrillisation of α -synuclein, preventing aggregates' extracellular toxic effect on PC12 cells³⁷.

Here, we showed in the ThT experiment that compound **1** could inhibit β -sheet assembly through non-covalent interactions such as hydrogen bonds, confirmed by TMS experiments. Since this technique arises to quantify and determine the dissociation constant (Kd) through a temperature gradient, we determined this value in 50 μ M.

The structure we observed in AFM experiments correspond to fibrils and rounded morphological elements resembling oligomers. In the presence of **1**, we found that the diameter ranges from 180 to 400 nm, suggesting that an accumulation of elements could occur instead of forming fibrils. The Raman spectra of aggregation control reveal that most of the amide signals are related to the β -sheet formation and CH_2-CH_3 deformation. In the case of treated aggregates in the presence of **1**, we found most spectra related to unfolded α -synuclein and CH_2-CH_3 deformation, suggesting that those elements could correspond to an off-aggregation pathway. It is crucial to consider that neurite outgrowth is essential for cells. Thus, to test the hypothesis that the aggregates treated with compound **1** are non-toxic to cells, we decided to resemble this process by inducing neurite-like structures in the presence of retinoic acid. Then, we externally added to the cell culture non treated and treated aggregates by **1**. In cells challenged with non-treated aggregates, most of them retract neurite outgrow, and the presence of non-treated aggregates provokes cell swelling. In the cells challenged with treated aggregates in the presence of **1**, the neurites remain to suggest a non-harmful effect over cell culture. Finally, docking simulation reveals that **1** prefers sites 2, 9, and 3/13 in the NMR solid-state α -synuclein structure.

Acknowledgements

The authors also thank Daniel Maturana and Carolina Carriel (NanoTemper, Sao Jose dos Campos, Brazil) for help with the thermophoresis assays.

Disclosure statement

The authors declare no conflict of interest.

Funding

Alberto Cornejo and Carlos Areche acknowledge Instituto Antártico Chileno (INACH) RT_18-19. Julio Caballero acknowledges funds of FONDECYT Regular # 1170718, Mario Simirgiotis FONDECYT Regular # 1180059, and Francisco Melo FONDECYT Regular # 1201013, and Fondecyt EQM130149 and USA2055-042031MH_POSTDOC projects are also acknowledged. Vanessa Torres acknowledges APP-1 2019.

ORCID

Mario Simirgiotis  <http://orcid.org/0000-0003-4552-3123>
Carlos Areche  <http://orcid.org/0000-0001-5246-1368>

References

- Lashuel HA, Hartley D, Petre BM, et al. Neurodegenerative disease: amyloid pores from pathogenic mutations. *Nature* 2002;418:291.
- Maroteaux L, Campanelli JT, Scheller RH. Synuclein: a neuron-specific protein localized to the nucleus and presynaptic nerve terminal. *J Neurosci* 1988;8:2804–15.
- Burré J, Sharma M, Tsetsenis T, et al. Alpha-synuclein promotes SNARE-complex assembly in vivo and in vitro. *Science* 2010;329:1663–7.
- Recchia A, Debetto P, Negro A, et al. Alpha-synuclein and Parkinson's disease. *FASEB J* 2004;18:617–26.
- Spillantini MG, Goedert M. Neurodegeneration and the ordered assembly of α -synuclein. *Cell Tissue Res* 2018;373:137–48.
- Appel-Cresswell S, Vilarino-Guell C, Encarnacion M, et al. Alpha-synuclein p.H50Q, a novel pathogenic mutation for Parkinson's disease. *Mov Disord* 2013;28:811–3.
- Recasens A, Dehay B, Bové J, et al. Lewy body extracts from Parkinson disease brains trigger α -synuclein pathology and neurodegeneration in mice and monkeys. *Ann Neurol* 2014;75:351–62.
- Danzer KM, Krebs SK, Wolff M, et al. Seeding induced by alpha-synuclein oligomers provides evidence for spreading of alpha-synuclein pathology. *J Neurochem* 2009;111:192–203.
- Bonifacio MJ, Torrao L, Loureiro AI, et al. Pharmacological profile of opicapone, a third-generation nitrocatechol catechol-O-methyl transferase inhibitor, in the rat. *Br J Pharmacol* 2015;172:1739–52.
- Scott LJ. Opicapone: a review in Parkinson's disease. *Drugs* 2016;76:1293–300.
- Rocha J-F, Falcão A, Santos A, et al. Effect of opicapone and entacapone upon levodopa pharmacokinetics during three daily levodopa administrations. *Eur J Clin Pharmacol* 2014;70:1059–71.
- Dehay B, Bourdenx M, Gorry P, et al. Targeting α -synuclein for treatment of Parkinson's disease: mechanistic and therapeutic considerations. *Lancet Neurol* 2015;14:855–66.
- Ehrnhoefer DE, Bieschke J, Boeddrich A, et al. EGCG redirects amyloidogenic polypeptides into unstructured, off-pathway oligomers. *Nat Struct Mol Biol* 2008;15:558–66.
- Simirgiotis MJ, Jiménez C, Rodríguez J, et al. New dammarane triterpenes from the aerial parts of *Ibicella lutea* grown in Argentina. *J Nat Prod* 2003;66:1586–92.
- Hoyer W, Antony T, Cherny D, et al. Dependence of alpha-synuclein aggregate morphology on solution conditions. *J Mol Biol* 2002;322:383–93.
- Scheuermann TH, Padrick SB, Gardner KH, Brautigam CA. On the acquisition and analysis of microscale thermophoresis data. *Anal Biochem* 2016;496:79–93.
- Cornejo A, Jimenez JM, Caballero L, et al. Fulvic acid inhibits aggregation and promotes disassembly of tau fibrils associated with Alzheimer's disease. *J Alzheimers Dis* 2011;27:143–53.
- Viklický V, Dráber P, Hašek J, Bártek J. Production and characterization of a monoclonal antitubulin antibody. *Cell Biol Int Rep* 1982;6:725–31.
- Draber P, Rubino S, Dráberová E, et al. A broad spectrum monoclonal antibody to alpha-tubulin does not recognize all protozoan tubulins. *Protoplasma* 1985;128:201–7.
- Tuttle MD, Comellas G, Nieuwkoop AJ, et al. Solid-state NMR structure of a pathogenic fibril of full-length human α -synuclein. *Nat Struct Mol Biol* 2016;23:409–15.
- Hsieh C-J, Ferrie JJ, Xu K, et al. Alpha synuclein fibrils contain multiple binding sites for small molecules. *ACS Chem Neurosci* 2018;9:2521–7.
- Friesner RA, Murphy RB, Repasky MP, et al. Extra precision glide: docking and scoring incorporating a model of hydrophobic enclosure for protein–ligand complexes. *J Med Chem* 2006;49:6177–96.
- Alzate-Morales JH, Vergara-Jaque A, Caballero J. Computational study on the interaction of N1 substituted pyrazole derivatives with B-Raf kinase: an unusual water wire hydrogen-bond network and novel interactions at the entrance of the active site. *J Chem Inf Model* 2010;50:1101–12.
- Velázquez-Libera JL, Rossino G, Navarro-Retamal C, et al. Docking, interaction fingerprint, and three-dimensional quantitative structure–activity relationship (3D-QSAR) of Sigma1 receptor ligands, analogs of the neuroprotective agent RC-33. *Front Chem* 2019;7:496.
- Jorgensen WL, Maxwell DS, Tirado-Rives J. Development and testing of the OPLS all-atom force field on conformational energetics and properties of organic liquids. *J Am Chem Soc* 1996;118:11225–36.
- Bowers KJ, Chow DE, Xu H, et al. Scalable algorithms for molecular dynamics simulations on commodity clusters. SC'06: Proceedings of the 2006 ACM/IEEE Conference on Supercomputing; IEEE; 2006:43.
- Biancalana M, Koide S. Molecular mechanism of thioflavin-T binding to amyloid fibrils. *Biochim Biophys Acta Proteins Proteomics* 2010;1804:1405–12.
- Wolff M, Mittag JJ, Herling TW, et al. Quantitative thermophoretic study of disease-related protein aggregates. *Sci Rep* 2016;6:1–10.
- Maiti NC, Apetri MM, Zagorski MG, et al. Raman spectroscopic characterization of secondary structure in natively unfolded proteins: alpha-synuclein. *J Am Chem Soc* 2004;126:2399–408.
- Koch JC, Bitow F, Haack J, et al. Alpha-synuclein affects neurite morphology, autophagy, vesicle transport and axonal degeneration in CNS neurons. *Cell Death Dis* 2015;6:e1811.
- Pujols J, Peña-Díaz S, Pallarès I, Ventura S. Chemical chaperones as novel drugs for Parkinson's disease. *Trends Mol Med* 2020;26:408–21.
- Dorsey ER, Bloem BR. The Parkinson pandemic—a call to action. *JAMA Neurol* 2018;75:9–10.
- Giasson BI, Murray IV, Trojanowski JQ, Lee VM. A hydrophobic stretch of 12 amino acid residues in the middle of alpha-synuclein is essential for filament assembly. *J Biol Chem* 2001;276:2380–6.
- Silva M, Caro V, Guzmán C, et al. Chapter 1 - α -Synuclein and tau, two targets for dementia. In: Atta-ur-Rahman, ed. *Studies in natural products chemistry*. Vol. 67. Elsevier; 2020:1–25. <https://doi.org/10.1016/B978-0-12-819483-6.00001-1>
- Zhu M, Rajamani S, Kaylor J, et al. The flavonoid baicalein inhibits fibrillation of alpha-synuclein and disaggregates existing fibrils. *J Biol Chem* 2004;279:26846–57.
- Zheng ZV, Cheung CY, Lyu H, et al. Baicalein enhances the effect of low dose Levodopa on the gait deficits and protects dopaminergic neurons in experimental Parkinsonism. *J Clin Neurosci* 2019;64:242–51.
- Di Giovanni S, Eleuteri S, Paleologou KE, et al. Entacapone and tolcapone, two catechol O-methyltransferase inhibitors, block fibril formation of alpha-synuclein and beta-amyloid and protect against amyloid-induced toxicity. *J Biol Chem* 2010;285:14941–54.